

Research Highlight

Chemical Vapor Deposition of Transition-metal Nanostructures

Keith Chan, Chris Doran, Jimmy Kan and Eric Fullerton
University of California, San Diego

As the dimensions of a material approach the nanoscale new physical and chemical properties emerge. Clear understanding of these properties and their new functionality will lead to emerging applications in diverse areas such as catalysis¹, fuel cells², thermoelectrics³, sensors⁴, batteries⁵, and magnetic devices.⁶ Chemical vapor deposition (CVD) techniques have been applied to achieve a broad range of nanostructured materials with a particular focus on the growth of nanowires (NWs). The most common and well-studied CVD methods for NW synthesis have focused on the elemental semiconductors Si and Ge, compound semiconductors including ZnO and InAs, as well as C nanotubes. The synthesis of these high-aspect-ratio materials typically relies on the vapor-liquid-solid (VLS) mechanism using foreign catalyst seeding and lattice-matched single-crystal substrates for morphological control and epitaxy-dependent vertically-oriented growth, respectively.

Research at CMRR has focused on extending CVD to new types of NW materials, particularly transition-metals and their oxides, to broaden their applications and impact. Furthermore the realization of many practical applications will require efficient and economical synthesis techniques that preferably avoid the need for templates or costly single-crystal substrates. Towards this end we have developed an efficient and economical single-step route for the reduction-type synthesis of nanostructured Ni materials using a thermal CVD.⁷ By tuning the CVD growth parameters we can synthesize Ni nanostructures including single-crystal cubes (Fig. 1) and horizontally- and vertically-oriented NW arrays (Fig. 2) and polycrystalline Ni/NiO core-shell NWs which all form atop untreated amorphous SiO₂||Si substrates.

In addition to the well-known uses of its magnetic behavior in various spin-based devices, nanostructured Ni and Ni-based materials are also critical components in many chemical engineering processes including such examples as the steam reformation of CH₄ in synthesis gas production and other similar applications utilizing the catalytic nature of transition-metal surfaces. Ni-based NWs in particular have high surface area-to-volume ratios and are capable of providing a high density of active sites for surface reactions thereby increasing the efficiency in such applications. Additionally, materials like the core-shell structured Ni-NiO NWs can serve as templates for further material deposition in cases where a non-interacting surface is desired.⁶

Shown in Fig. 2 are two of the synthesized Ni NW phases: vertically oriented NWs (Fig. 2a) and horizontally oriented NWs (Fig. 2b). X-ray and electron diffraction show that the NWs are single-crystal, are oriented along <001> crystallographic direction with a face-centered cubic unit cell of 0.352 nm consistent with bulk Ni and are atomically smooth. The NWs can be grown with diameters ranging from 50 to 300 nm and lengths up to 5 μ m for vertical NWs (Fig. 1a) and 80 μ m for horizontal NWs (Fig. 2b). Vertical NW diameter and growth density can be further controlled through temperature adjustment as seen in Figs. 2c and 2d. Figure 2c are 100-nm diameter wires with a relatively low density of 0.1 NW/ μ m² while Fig. 2d are 250-nm diameter NWs with a higher density of 0.3 NW/ μ m².

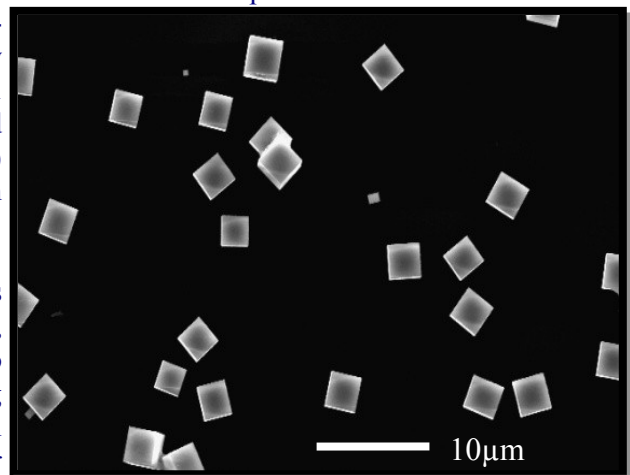


Figure 1: Single-crystal Ni cubes formed on SiO₂ coated Si substrates.

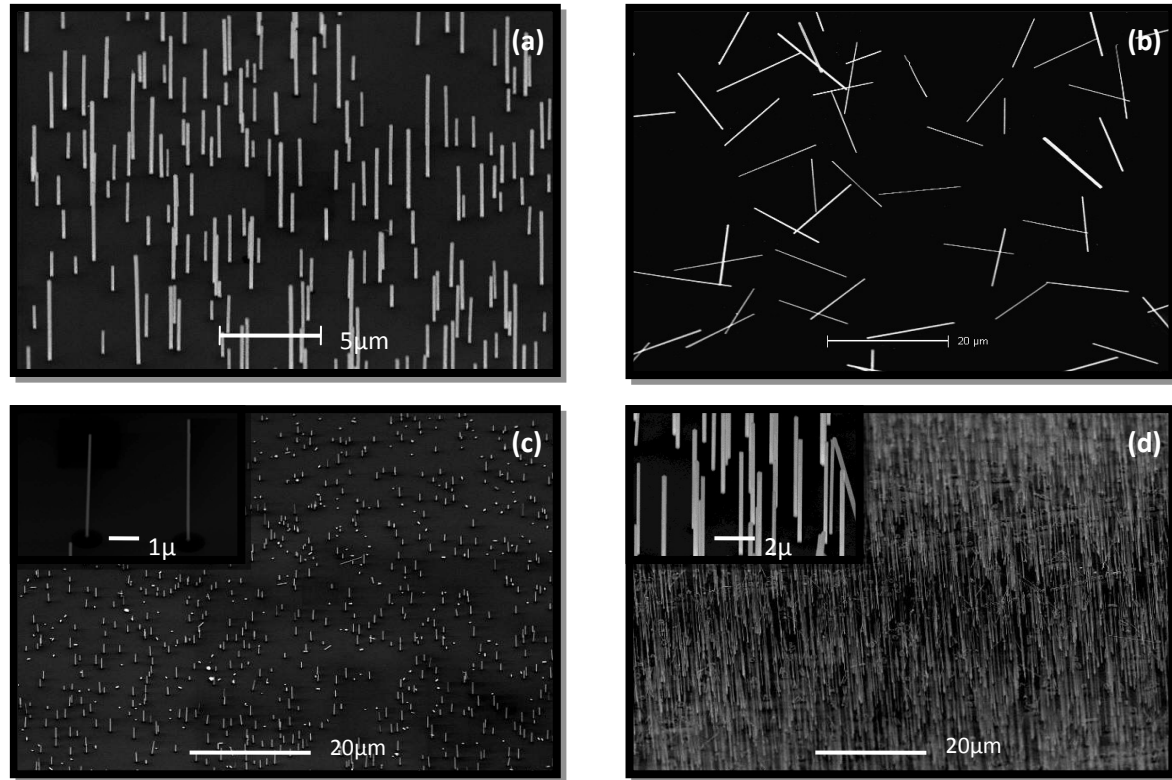


Figure 2: SEM images of as-grown Ni NW arrays with (a) vertical orientation grown at 650°C, (b) horizontal orientation grown at 700°C and vertically oriented NWs with (c) low density and diameter near 100nm grown at 630°C and (d) high density and diameter near 250nm grown at 675°C.

A detailed formation mechanism for the vertically-oriented, single-crystal NW phase is given in Ref. 7 which relies on a laterally confined layer of Si-based material for growth mediation. Preferential accumulation of Ni adatoms at Si-rich growth sites leads to anisotropic crystallization proceeding along a single direction. The Si responsible for NW formation is likely released from the cleaved sidewalls of the $\text{SiO}_2\text{||Si}$ substrates. By further controlling the precursor moisture content and temperature a broad range of phases can be formed.

We characterized the magnetic response of individual NWs by magneto-transport measurements (Fig. 3) and x-ray photoemission electron microscopy (Fig. 4). The anisotropic magnetoresistance (AMR) of ferromagnetic materials depends on the relative angle between the magnetization direction and the current flow. Shown in Fig. 3 is the AMR behavior of a 100-nm-diameter vertical NW as measured at 10 K with the applied field both parallel and perpendicular to the NW axis. The AMR curves are nearly reversible (i.e. independent of field history) with only small regions of irreversibility. The NW resistance at $H_{\text{applied}} = 0$ Oe is intermediate between the parallel and perpendicular states indicating a remanent state with an angle of magnetization ~ 45 degrees to the wire axis. To understand the NW magnetic behavior we have modeled the magnetic response of a $<001>$ -oriented single-crystal NW using micromagnetic simulations and the bulk properties of Ni. Results of the AMR calculations are shown in Fig. 3 which reproduces all of the observed features of the measured AMR data.

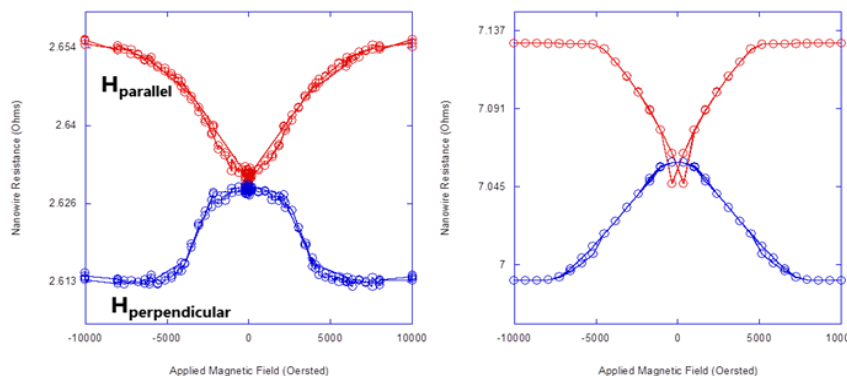
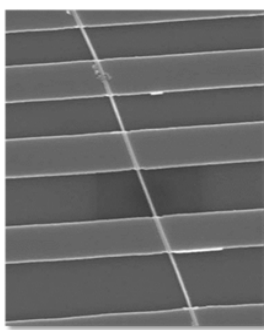


Figure 3: We use magneto-transport measurements of individual Ni NWs to probe their magnetic response to field. The left image is an individual wire with leads where we measure the resistance as a function of applied field parallel and perpendicular to the wire axis. The left graph is the measured data and the right graph is the results of micromagnetic simulations.

The simulations suggest a complex domain behavior that forms during reversal. This behavior results from the competing shape anisotropy of the NW, which favors magnetization along the NW axis, and the magnetocrystalline anisotropy, which favors magnetization along the $<111>$ crystallographic direction. This competition results in the formation of stripe domains down the wire shown in the top image of Fig. 4. To confirm the behavior we imaged the domain pattern of individual wires (Fig. 4 bottom image) which agrees quantitatively with the micromagnetic results and shows the wires are behaving as expected for a single-crystal NW.

In conclusion we have developed a simple CVD approach from metal-halide precursors to form and control distinct nanostructured growth phases of Ni. Of particular importance is the establishment of a detailed methodology concerning the growth of NW growth phases which successfully relates specific experimental growth parameters, underlying formation mechanisms, and electrical and magnetic properties. This study of Ni nanostructure growth phases readily lends itself to a generalized approach for nanostructure growth of transition metals that can be applied to a broad range of nanotechnologies.

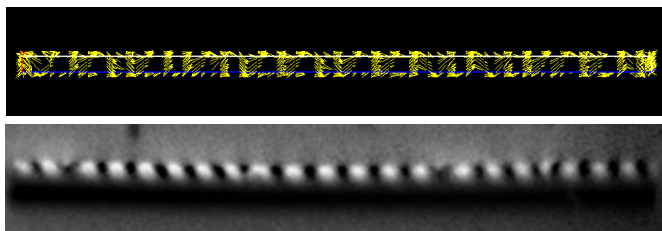


Figure 4: Magnetic domain images (top) for a single-crystal Ni NW compared to magnetic imaging (below).

1. Beebe, T.P.; Goodman, D.W.; Kay, B.D.; Yates, J.T. *J. Chem. Phys.* **1987**, 87(4), 2305-2315.
2. Asazawa, K.; Sakamoto, T.; Yamaguchi, S.; Yamada, K.; Fujikawa, H.; Tanaka, H.; Oguro, K. *J. Electrochem. Soc.* **2009**, 156(4), B509-B512.
3. Boukai, A.I.; Bunimovich, Y.; Tahir-Kheli, J.; Yu, J.K.; Goddard, W.A.; Heath, J.R. *Nature* **2008**, 451(7175), 168-171.
4. Shibli, S.M.A.; Beenakumari, K.S.; Suma, N.D. *Biosens. Bioelectron.* **2006**, 22(5), 633-638.
5. Chan, C.K.; Peng, H.L.; Liu, G.; McIlwrath, K.; Zhang, X.F.; Huggins, R.A.; Cui, Y. *Nat. Nanotechnol.* **2008**, 3(1), 31-35.
6. Chan, K.T.; Doran, C.; Shipton, E.G.; Fullerton, E.E. *IEEE Trans. Magn.* **2010**, 46(6), 2209-2211.
7. Chan, K.T.; Kan, J.J.; Doran, C.; Lu O.; Smith, D.J.; Fullerton, E.E., *Nano Lett.* **2010**, 10, 5070.